

## Development and Verification of Electrokinetic Injection Logical Control Mode in Microfluidic Device

Yu-Jen Pan

Department of Supply Chain Management, National Kaohsiung University of Science and Technology, Taiwan

Received 07 September 2023; revised 20 October 2023; accepted 15 January 2024

This study presents a methodology for discretely injecting sample flows propelled by electroosmosis within a microfluidic device. The inquiry begins by analyzing the buffer distance required to hinder diffusion between successive distinct sample entities. Following this, a systematic formulation is developed to identify operational parameters that ensure the comprehensive deposition of the specimen segment into the assigned discharge reservoir. The results indicate that precise manipulation of voltages applied to the microfluidic device's various inlet and outlet channels enables the automatic and continuous delivery of samples with varying lengths to specified outlet reservoirs. Experimental evidence supports the claim that applying a voltage to the non-receiving reservoir during injection enhances the microfluidic device's injection performance by preventing sample leakage. Furthermore, findings from both experimental and numerical analyses suggest that optimizing the spatial configuration of the outlet channels enhances the overall efficiency of the injection process.

**Keywords:** Diffusion, Electroosmosis, Electroosmotic flow, Rhodamine, Sequential injection

### Introduction

In a standard bio-analytical assay conducted with a microfluidic device, the setup includes several entry points and exit points. During bio-analytical analyses, it becomes crucial to precisely direct the flow of sample fluids to specific outlet ports. This precision is essential for delivering accurate quantities of fluids to reservoirs where biochemical reactions occur. Numerous studies in the past have focused on the development of flow-switching mechanisms in microfluidic systems. Various designs have been proposed for microfluidic devices with integrated flow-switching functionalities, where an active structure is incorporated into fluid-carrying microchannels. In microfluidic channels, fluid flow is commonly induced by either external pressure or electroosmotic phenomena in response to externally applied electric fields.<sup>1-3</sup> Among these approaches, Electroosmotic Flow (EOF) stands out as a preferred method due to its elimination of the necessity for mechanical moving parts and its capability to precisely manipulate very small sample volumes through a customized voltage modulation strategy. Certain microfluidic devices, intentionally designed for bioprocessing studies, leverage electrokinetic

forces. These devices employ electrokinetic operation methods to synergize with electrokinetic instability, ensuring effective mixing.<sup>4</sup>

Sequential Injection Analysis (SIA) is a technique in analytical chemistry that serves as an alternative to Flow Injection Analysis (FIA). It is frequently employed in microfluidic devices that are microfabricated on chips. The sequential injection technique has found applications in biochemical analysis within the context of microfluidic devices.<sup>5-7</sup> The sequential injection method is demonstrated to be effective in enhancing mixing within micro-channels. A field switching strategy was employed by Coleman *et al.*, who implemented a symmetric sequential injection technique. This approach facilitated the injection of various fluids into a geometry featuring an expansion chamber, resulting in significantly improved mixing efficiency.<sup>8</sup> The SIA technique used in the diet field, for example, the determination of lead in vegetables.<sup>9</sup> The water quality is always the focus. Lai *et al.* developed an SIA device for determination of metal in environmental water.<sup>10</sup> A miniature in-situ multi-parameter detector for water quality assessment has been devised, amalgamating SIA with continuous spectral detection methods.<sup>11</sup>

The current study proposes a technique for logically injecting a single sample in a microfluidic device featuring multiple inlet and outlet channels. By

exploiting the concepts of electrokinetic focusing and microfluidic delay loops and applying an appropriate voltage control scheme, it is shown that discrete samples of varying length (i.e. variable volume) can be automatically dispensed to the designated reservoir channels on a continuous basis. The qualitative demonstration reveals that the injection performance of the microfluidic device can be improved through the optimization of the geometrical configuration of the outlet channels. Furthermore, the imposition of voltage on the outlet reservoir not receiving the sample during the injection procedure efficiently mitigates sample leakage.

## Materials and Methods

### Generation of Discrete Sample in a Channel

Presented in the Fig. 1 is a contemporary microfluidic device, with three designated input channel outlets identified as P, Q, and R. The device also features two output reservoirs labeled as a and b. In the operational context, the introduction of the sample occurs through reservoir Q. The sample undergoes refinement through enveloping buffer flows originating from P and R, and is subsequently directed to outlet channel a or b through a straightforward voltage control scheme. The Distance line (D-line) is crafted to regulate the length of the buffer flow. An increase in the D-line corresponds to

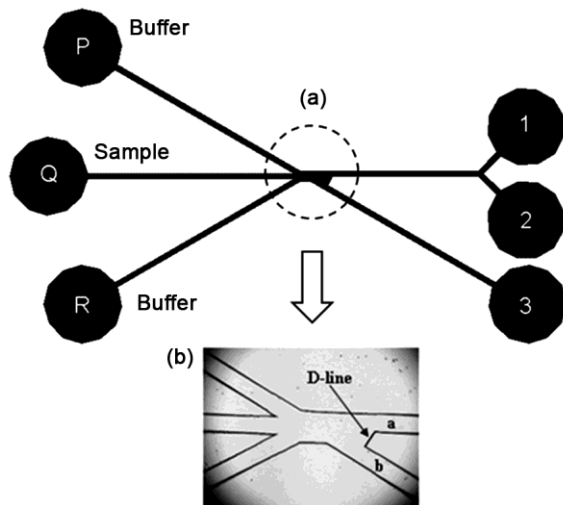


Fig. 1 — (a) Schematic depiction of the proposed microfluidic device tailored for sequential injection. Notably, the channel dimensions include a width of 200  $\mu\text{m}$ , a depth of 20  $\mu\text{m}$ , and individual reservoirs with a diameter of 3000  $\mu\text{m}$ . Inlet reservoirs are designated as P, Q, and R, whereas outlet channels are identified as a and b; and (b) Enhanced view focusing on the chamber in proximity to the junction between the inlet and outlet channels

a lengthening of the time (delay time) needed for the movement of the specimen within the channel, transitioning from channel-b to channel-a. In the sequential injection process, it is crucial to introduce a specific volume of intermediary solution between successive distinct aliquots to prevent convective dispersion during transportation. Therefore, Fick's law<sup>12</sup> of mass diffusion is utilized to compute the buffer extent ( $\Delta X$ ) during the time it takes for the segments to move from the entry point of the afflux channel to the exit. The computation of the buffer length is conducted as follows:

$$\Delta X \approx 6.4\sqrt{Dt} \quad \dots (1)$$

The sample's diffusion coefficient, denoted by  $D$ , stands as a pivotal parameter in this context. It's noteworthy that Rhodamine B serves as the sample in the current study, hence  $D = 3 \times 10^2 (m^2/s)$ . In the course of experimental scrutiny, the duration for the sample to navigate through the injection channel, spanning from the inlet to the outlet, hinges on the specific geometric arrangement. For the instances documented in this study, the estimated transit time is denoted as  $t=20$  seconds. Consequently, to forestall diffusive mixing between the two successive sample plugs prior to reaching the outlet reservoirs, the buffer is required to span a length of 156.76  $\mu\text{m}$ .

Referring to Fig. 1, the commencement of the sequential injection process involves grounding channel-b and applying voltages to channels P, Q, and R, while simultaneously keeping the exit reservoirs in an unobstructed circuit state. This careful manipulation results in the concentration and guidance of the specimen flow into channel-b by the paired enveloping flows. Subsequently, the grounding condition transitions from channel-b to channel-a, facilitating an immediate flow of the buffer into channel-a. However, the sample requires a finite amount of time (referred to hereafter as the delay time) to reverse its direction of travel in channel-b and to change its flow direction to channel-a along the distance line (i.e. the microchannel wall between the inlet of channel-b and that of channel-a, see Fig. 1b is introduced into the inlet of channel-a). Upon integration with the buffer stream in a channel, the sample undergoes a transition marked by the return of grounding from a to b. This redirection facilitates the re-entry of the sample into b channel. Subsequently, a channel is grounded, facilitating the ingress of the buffer solution into a channel. This, in turn, induces

the sample to once again modify its flow direction along the distance line (D-line). As a result, the delivery pathway showcases two discrete sample entities identified as stopper A and stopper B, respectively. These plugs are distinctly separated by a volume of buffer solution. The length of the buffer solution is conspicuously dictated by the delay time, while the lengths of the two sample plugs are contingent upon the durations during which the respective outlet reservoirs are grounded.

**Delivering Discrete Sample to a Designated Reservoir**

In the sequential injection process, it is crucial to ensure the full dispensation of both plugs into their assigned receptacles. In other words, no residual plug should be left within the injection channel. This requires a careful specification of the ground times of the outlet reservoirs and a knowledge of the delay time of the microfluidic chip. We design two reservoirs in the outlet channel-a for collection two different length of the sample, as shown in Fig. 1. In practice, an appropriate voltage control scheme can be derived based on the following formula:

$$L \leq V(t_1M + t_2M) \leq L + X \quad \dots (2)$$

where,  $L$  is a channel length ( $\mu\text{m}$ );  $X = TV$  is the length of the buffer, where  $V$  is the flow velocity in channel-a and  $T$  is the delay time;  $t_1$  is the duration during which reservoir 1 is connected to ground;  $t_2$  is the duration during which reservoir 2 is connected to ground; and  $M$  and  $N$  are the number of times for which reservoirs 1 and 2 are grounded in one complete injection cycle. Consequently,  $Vt_1$  gives the length of plug A + buffer (i.e.  $\alpha$ ),  $Vt_2$  is the length of plug B + buffer (i.e.  $\beta$ ), and  $Vt_1M + Vt_2N$  is the total length of the sample string produced in one complete cycle.

As described in the following, we show two usable operation modes by Eq. 2. The two operation conditions are presented in Table 1. The total length of one complete cycle for the case 1 is  $4000 \mu\text{m}$ , which is equal to the length of channel-a, and that for the case 2 is equal to the Right Hand Side (RHS) of Eq. 2. As an example for the case 1, consider the case where  $t_1$  and  $t_2$  are specified as 1.5 sec and 1 sec, respectively,  $M$  is assigned a value of 4 and  $N$  is assigned a value of 2. In this case, the total length of the sample string is  $4000 \mu\text{m}$ , which is equal to the Left Hand Side (LHS) of Eq. (2). Therefore, as shown in Fig. 2a, plug A

Table 1 — Two operation conditions for delivering different sample length to a designated reservoir

	$t_1$	$t_2$	$m_1$	$m_2$	$V(t_1m_1 + t_2m_2)$
Case 1	1.5	1	4	2	4000
Case 2	1.5	1.15	4	2	4150

Note:  $L = 4000 \mu\text{m}$ ;  $V = 500 \mu\text{m/s}$ ;  $T = 0.3 \text{ sec}$ ; the buffer length:  $X = V \times T = 150 \mu\text{m}$

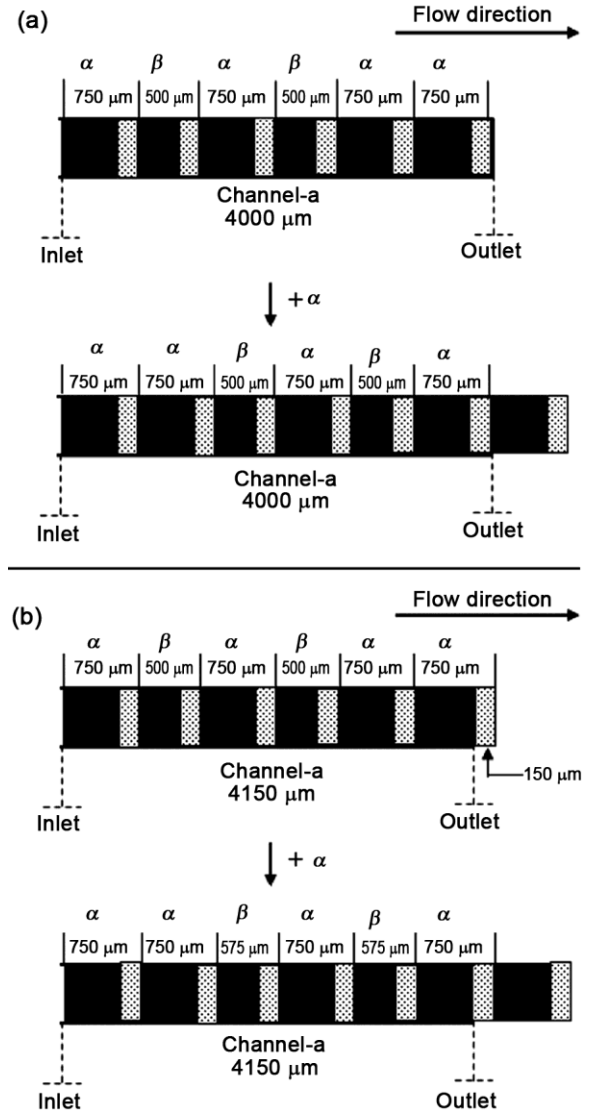


Fig. 2 — (a) The sequential injection process, the total length of the sample is  $4000 \mu\text{m}$ ; Consequently, plug  $\alpha$  is dispensed fully into the outlet reservoir following the next dispensing process; and (b) The sequential injection process, the total length of the sample is  $4150 \mu\text{m}$ ; Consequently, plug  $\alpha$  is dispensed fully into the outlet reservoir following the next dispensing process

flows completely into the outlet reservoir leaving no residue in the injection channel following the next dispensing process. Similarly for the case 2, consider the case where  $t_1 = 1.5 \text{ sec}$ ,  $t_2 = 1.15 \text{ sec}$ ,

M = 4 and N = 2. In this case, the total length of the sample string is 4150  $\mu\text{m}$ , which is equal to the RHS of Eq. (2). Therefore, as shown in Fig. 2b, plug A flows completely into the outlet reservoir.

The discussions above have focused on the dispensing of single samples into the outlet reservoir. However, in practice, the sequential injection procedure is a continuous process, in which the dispensing of a single sample plug into an outlet reservoir is accompanied by the introduction of a sample plug of equivalent length into the inlet of the injection channel. Consider the sample sequence shown in the upper schematic in Fig. 2a. As shown, the sequential injection process produces the sample sequence "αβαβα" in channel-a, where α comprises the sample (600  $\mu\text{m}$ ) and a buffer of length 150  $\mu\text{m}$ , and β comprises the sample (350  $\mu\text{m}$ ) and a buffer of length 150  $\mu\text{m}$ . These plugs have total length of 4000  $\mu\text{m}$  and therefore completely fill the injection channel. Assume that α is to be dispensed into reservoir 1 and β into reservoir 2. The operation procedure is illustrated in Fig. 3 as the following step-by-step process:

Step 1: Ground reservoir 1. This causes plug A at the outlet of channel-a to flow into reservoir 1 and induces the flow of buffer and a new plug of

sample A into the inlet of the injection channel (i.e. the channel now contains αβαβα).

Step 2: Repeat Step 1 (the channel now contains ααβαβ).

Step 3: Ground reservoir 2. This causes β at the outlet of channel-a to flow into reservoir 2 and induces the flow of buffer and a new plug of sample B into the inlet of channel-a (i.e. the channel now contains βααβα).

Step 4: Repeat step 1 (the channel now contains αβαααβ).

Step 5: Repeat step 3 (the channel now contains βαβααα).

Step 6: Repeat step 1 (the channel now contains αβαβαα).

It is evident that through the systematic execution of this procedural sequence, the channel encapsulates the identical sample string as originally contained within channel-a. Alternatively, the cyclic and continuous implementation of the sequential injection protocol becomes viable upon the specification and configuration of requisite operational conditions. Although the sample string "αβαβαα" is presented for illustration purposes here, in practice, any sample string (e.g. ααααββ", "ααββαα", "αββααα", and so forth) can be obtained simply by modifying the sequence in which reservoirs 1 and 2 are grounded.

**Electrical Circuit Representation**

The operating states of the current microfluidic device can be represented using an electrical circuit analogy.<sup>13</sup> The sequential injection process is controlled using two power supplies. Power supply 1 applies a voltage continuously to the three inlet reservoirs and grounds or isolates the outlet reservoirs as and when required to achieve the specified sample injection sequence. Concurrently, as clarified later, Power Supply 2 applies a voltage (220 V) to the reservoir not receiving the sample during the injection process to alleviate the risk of sample leakage. The three-state voltage control scheme employed to implement the sequential injection process is summarized in Table 2. State 1, 2 & 3 of electrical circuit is represented as Fig. 4a, b & c respectively. The electrical resistance of a solution is given by the following expression:

$$R = \frac{\rho L}{A_c} \dots (3)$$

where, ρ is the electrical resistance of the solution, L is the length of channel, A<sub>c</sub> is the cross-sectional area

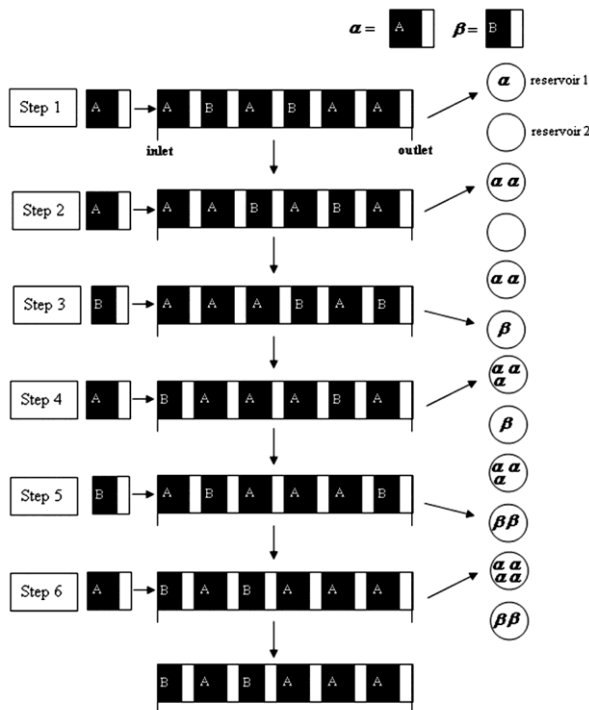


Fig. 3 — The complete process of a cycle. Plug α and plug β are delivered to reservoir 1 and reservoir 2, respectively

Table 2 — Three-state voltage control scheme

State	Inlet P, Q, R	Outlet		
		1	2	3
State 1	550V	220V	G	I
State 2		I	I	G
State 3		G	220V	I

I: isolation; G: ground

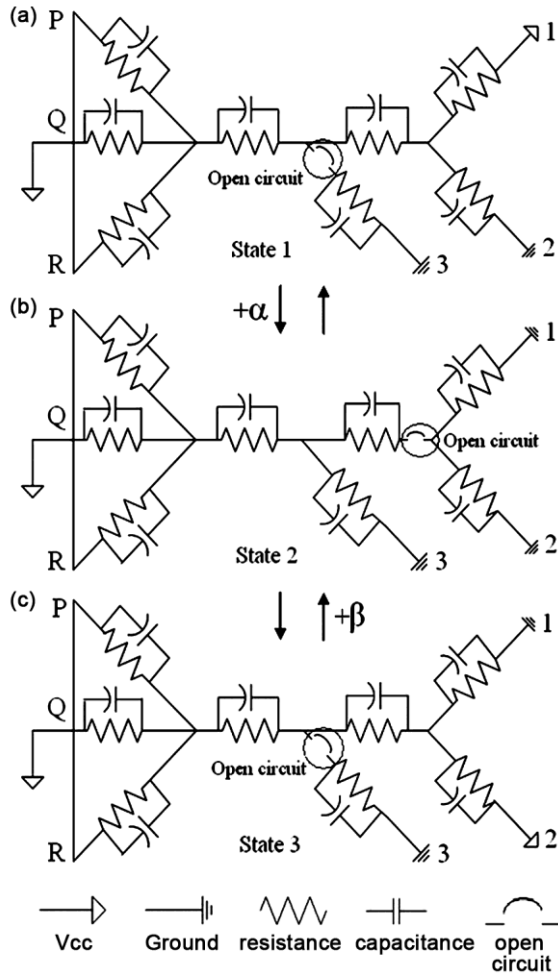


Fig. 4 — Electrical network representation of a microfluidic device: (a) State 1, (b) State 2, (c) State 3; the electrical circuit symbols are introduced and defined above

of channel. Electrical double layer can be expressed by the effective capacitance. It is given by  $(C_{eff})^{-1} = (C_{st})^{-1} + (C_{dl})^{-1} + (C_{wall})^{-1}$  ... (4)

where,  $C_{eff}$  is the effective capacitance,  $C_{st}$  is the capacitance of Stern layer,  $C_{dl}$  is the capacitance of diffuse layer,  $C_{wall}$  is the capacitance of channel wall. In the experiment, the ratio of the thickness of double layer (10 nm ~ 100 nm) to that of channel (200 μm) is

more than 1:2000. The effect of capacitance is very weak so that it can be ignored. We can assume all the capacitances as open circuit in electrical circuit representations.

As shown, in State 1, reservoir 3 is isolated (i.e. an open circuit is imposed), reservoir 2 is grounded and reservoir 1 is supplied with 220 V. As a result, the sample flows into reservoir 2. In State 2, reservoirs 1 and 2 are both isolated and reservoir 3 is grounded. Consequently, the sample flows into reservoir 3. Finally, in State 3, reservoir 3 is isolated, reservoir 1 is grounded and reservoir 2 is supplied with 200 V. Thus, the sample flows into reservoir 1.

**Materials and Reagents**

The sodium calcium glass substrate was procured from Fair & Cheer Inc., and the ultraviolet (UV) cured epoxy resin was obtained from Opas UV Technologies Co., Ltd. Acetone, sourced from Nihon Shiyaku Industries, served as a solvent in the epoxy resin developer solution. The experimental samples currently under investigation encompass a 10 mM sodium borate buffer solution (pH = 9.0) and a 10 mM sodium borate buffer solution augmented with Rhodamine B ( $10^{-4}$  M).

**Microfluidic Device Fabrication**

The current investigation employed glass substrates for the fabrication of the microfluidic device. The comprehensive details of the fabrication process are available in the literature, as referenced by Lin *et al.*; therefore, only a concise overview of the fabrication procedure is provided herein. The substrate underwent an initial cleaning process by infiltration into boiling Piranha solution for a duration of 10 minutes. Subsequently, it was thoroughly rinsed with deionized (DI) water and dried using high-purity nitrogen gas. Subsequently, the substrate underwent a thermal treatment on a hot plate set at 100°C to ensure the thorough removal of residual water droplets from its surface. The substrate was coated with a positive photoresist layer having a thickness of 7 μm, followed by a subsequent soft baking process. A conventional lithography process was performed using photomasks designed using AutoCAD 2000 layout software and printed using a high-resolution laser printer. Ultimately, employing a mask aligner, the positive photoresist (PR) coating underwent an exposure process for a duration of 26 seconds with an exposure dose specific to the G-line wavelength. The exposed coating was developed via immersion in a development solution for 135 sec. Having rinsed the

substrate in DI water, it was dried using nitrogen gas and then baked at 150°C for 10 min on a hot plate. Finally, the substrate was immersed in a BOE (buffered oxide etch) solution for 20 min to form microchannels with a depth of 20  $\mu\text{m}$ . Meanwhile, a blank substrate was drilled with via holes, lightly bonded with the lower patterned substrate using DI water and then fusion bonded on a hot plate. In the bonding process, the temperature was increased from 25°C to 680°C over a period of eight hours and was then gradually cooled back down to 25°C over the course of approximately 24 hours.

#### Detection System

During the experimental trials, manipulations of fluid samples within the microfluidic device were monitored utilizing fluorescence induced by a mercury lamp, with observation facilitated through a charge-coupled device camera (CCD). Electrokinetic propulsive forces were generated employing a high-voltage electrical source. Experimental images were captured using an optical microscope, subjected to spectral filtering, and subsequently quantified through the CCD device.

## Results and Discussion

#### Focusing Sample Flow

The injection performance of the developed microfluidic device is largely dependent on the value of the driving voltage applied to the inlet reservoirs (i.e. P, Q and R) and the ground time specified for reservoir 3. Considering the scenario where a voltage of 200 V is applied to the input chambers P, Q, and R, and a ground time of 1 second is assigned to chambers 3. Although the ground time of reservoir 3 is sufficient for the sheath flows to direct the sample toward channel-b, the comparatively low value of the driving voltage results in a weak focusing effect, and hence the sample diffuses along the D-line and mixes with the buffer. The diffusion of the sample along the D-line effectively reduces the delay time, and hence the distinction between the buffer and the sample is lost within channel-a (Fig. 5a). To ensure a clear separation of the individual sample plugs within channel-a, it is necessary to specify both an appropriate ground time for reservoir 3 and a sufficient value of the driving voltage applied at the inlet reservoirs such that a strong focusing effect can be achieved. A driving voltage of 550 V and a ground time of 1 seconds prevent mixing of the buffer and the sample prior to their entry into channel-a. As a result, the sequential introduction of the sample and buffer into

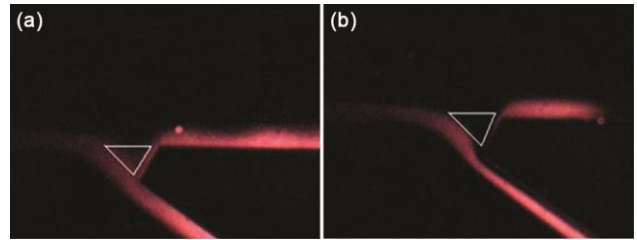


Fig. 5 — (a) The diffusion of the sample reduces the distinction between the buffer and the sample; and (b) Discrete sample plugs can be generated by applying a focusing effect

channel-a is facilitated by alternating grounding between reservoir 3 and reservoirs 1 or 2, as illustrated in Fig. 5b, as opposed to their simultaneous entry.

#### Effect of D-line

As mentioned earlier, the buffer solution continuously flows into channel-a during the delay time, which represents the duration for the sample to diffuse along the D-line towards the inlet of channel-a. Consequently, the distance line (D-line) critically influences the separation of buffer lengths between consecutive sample plugs within the injection channel. In the absence of a D-line in the microfluidic device, the delay time is notably short, providing inadequate time for buffer to be introduced between consecutive sample plugs. However, as depicted in Fig. 5, the inclusion of a D-line prolongs the delay time, enabling an ample amount of buffer to be transported into a channel between two successive samples.

#### Generating Variable-Volume sample

As mentioned earlier, the extent of the introduced sample section into a channel can be readily regulated by adjusting the duration of grounding for reservoir 1 or 2. For the purpose of exemplification, let's contemplate allocating a grounding duration of 1 second to reservoir 1. After grounding this reservoir, the sample flows into channel-a for a total time of  $(1-T)$  second, where  $T$  is the delay time (i.e. the time for which the buffer flows along D-line into channel-a). Assume further that reservoir 2 is assigned a ground time of 0.7 sec. Hence, the sample flows into channel-a for a time of  $(0.7-T)$  sec. In both cases, the length of the sample is given by  $V \times (t - T)$ , where  $V$  is the flow velocity in a channel,  $t$  is the ground time and  $T$  is the delay time. The difference in the durations of grounding applied to the two reservoirs leads to a significant variation in the length (and consequently the volume) of the two segments.

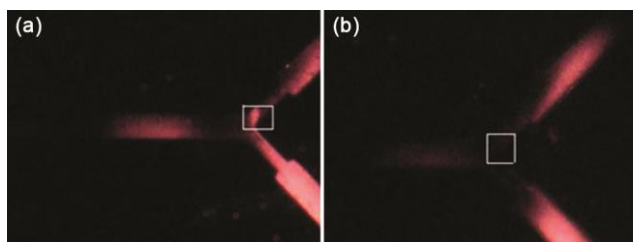


Fig. 6 — (a) The sample flow is directed into reservoir 2, a small amount of sample leaks into the channel connecting the injection channel with reservoir 1 as a result of diffusion; and (b) When applying a voltage to reservoir 1, the entire sample is dispensed into reservoir 2

### Suppression of Sample Leakage

Sample leakage is an undesired phenomenon. For example, as shown in Fig. 6a, when reservoir 2 is grounded and reservoir 1 is isolated (i.e. an open circuit condition is applied), the majority of the sample plug flows into reservoir 2 and a small amount of sample leaks into the channel connecting the injection channel with reservoir 1 as a result of diffusion. Therefore, to suppress this leakage effect, an appropriate voltage is applied to reservoir 1 when reservoir 2 is grounded (see Table 2, State 1). As shown in Fig. 6b, the application of this voltage suppresses the diffusion of the sample into the channel leading to reservoir 1, and ensures that the entire sample plug is dispensed into reservoir 2.

### Conclusions

The study initially formulates an analytical approach to determine the necessary operating parameters for a logically guaranteed injection, ensuring the complete deposition of a sample plug into the designated outlet reservoir. Subsequently, the study experimentally demonstrates a voltage control scheme facilitating the electrokinetic injection of discrete samples in a microfluidic chip with multiple inlet and outlet ports. The results demonstrate that the automated and continuous dispensing of sample plugs into designated outlet reservoirs can be achieved by accurately specifying the intensity and duration of applied voltages to the inlet and outlet channels.

Furthermore, the study reveals that optimizing the geometry of the outlet channels and applying voltage to the non-receiving outlet reservoir during the dispensing process can enhance the dispensing performance of the microfluidic device and suppress sample leakage. This logically operated device can be seamlessly integrated with other microfluidic components to create a novel or renewable energy system.

### Conflict of Interest

The authors declare no conflict of interest.

### References

- Bandopadhyay A, Mandal S & Chakraborty S, Capillary transport of two immiscible fluids in presence of electroviscous retardation, *Electrophoresis*, **38** (2017) 747–754, <https://doi.org/10.1002/elps.201600395>.
- Li H, Wong T N & Nguyen, N Y, Semi-analytical model of mixed electroosmotic/pressure driven two immiscible fluids with curved interface, *Micro Nanosyst*, **3** (2011) 296–310, doi: 10.2174/1876402911103040296.
- Maruthi P K, Subadra N & Srinivas M A S, Thermal effects of two immiscible fluids in a circular tube with nanoparticles, *J Nanofluids*, **6** (2017) 105–119, <https://doi.org/10.1166/jon.2017.1302>.
- Dubey K K, Gupta A & Bahga S S, Coherent structures in electrokinetic instability with orthogonal conductivity gradient and electric field, *Phys Fluids*, **29** (2017) 092007, <https://doi.org/10.1063/1.5003409>.
- Qiao J, Hou X, Steier P & Golser R, Sequential injection method for rapid and simultaneous determination of  $^{236}\text{U}$ ,  $^{237}\text{Np}$ , and Pu isotopes in seawater, *Anal Chem*, **85** (2013) 11026–11033, <https://doi.org/10.1021/ac402673p>.
- Silvestre C I, Pinto P C, Segundo M A, Saraiva M L & Lima J L, Enzyme based assays in a sequential injection format: A review, *Anal Chim Acta*, **689** (2011) 160–177, <https://doi.org/10.1016/j.aca.2011.01.048>.
- Šrámková I, Amorim C G, Sklenářová H, Montenegro M C, Horstkotte B, Araújo A N & Solich P, Fully automated analytical procedure for propofol determination by sequential injection technique with spectrophotometric and fluorimetric detections, *Talanta*, **118** (2014) 104–110, doi: 10.1016/j.talanta.2013.09.059.
- Coleman J T, McKechnie J & Sinton D, High-efficiency electrokinetic micromixing through symmetric sequential injection and expansion, *Lab on a Chip*, **6** (2006) 1033–1039, <https://doi.org/10.1039/B602085B>.
- Wonganan T, Chaiyasing K, Liawruangrath B, Rannurags N & Liawruangrath S, Development of sequential injection analysis for the determination of lead in vegetables, *Chiang Mai J Sci*, **48** (2022) 1116–1128, doi: 10.12982/CMJS.2022.069.
- Lai Z W, Lin F Y, Qiu L H, Wang Y R, Chen X & Hu H, Development of a sequential injection analysis device and its application for the determination of Mn(II) in water, *Talanta*, **211** (2020) 120752, <https://doi.org/10.1016/j.talanta.2020.120752>.
- Li W, Wang L M, Cheng L & Cheng H Q, Sequential Injection-continuous spectroscopy based multi-parameter method for water quality analysis, *Spectrosc Spect Anal*, **41** (2021) 612–617, [http://dx.doi.org/10.3964/j.issn.1000-0593\(2021\)02-0612-06](http://dx.doi.org/10.3964/j.issn.1000-0593(2021)02-0612-06).
- White F, *Viscous fluid flow*, 3rd edn, (McGraw-Hill: New York, U.S.) 1974.
- Chatterjee A N & Aluru N R, Combined circuit/device modeling and simulation of integrated microfluidic systems, *J Microelectromech Syst*, **14** (2005) 81–95, <https://doi.org/10.1109/JMEMS.2004.839025>.
- Lin C-H, Lee G-B, Lin Y-H & Chang G-L, A fast prototyping process for fabrication of microfluidic systems on soda-lime glass, *J Micromech Microeng*, **11** (2001) 726–32, doi: 10.1088/0960-1317/11/6/316.